

Molecular Coolers: The Case For [Cu^{II}₅Gd^{III}₄]

Stuart K. Langley,^a Nicholas F. Chilton,^a Boujemaa Moubaraki,^a Thomas Hooper,^b Euan K. Brechin,^{*b} Marco Evangelisti^{*c} and Keith S. Murray^{*a}

Received (in XXX, XXX) Xth XXXXXXXXXX 200X, Accepted Xth XXXXXXXXXX 200X

5 First published on the web Xth XXXXXXXXXX 200X

DOI: 10.1039/b000000x

The use of triethanolamine (teaH₃) in 3d/4f chemistry produces the enneanuclear cluster compound [Cu^{II}₅Gd^{III}₄O₂(OMe)₄(teaH)₄(O₂CC(CH₃)₃)₂(NO₃)₄]·2MeOH·2Et₂O (1·2MeOH·2Et₂O) whose molecular structure comprises a series of vertex- and face-sharing {Gd^{III}Cu^{II}₃} tetrahedra.

10 Magnetic studies reveal a large number of spin states populated even at the lowest investigated temperatures. Combined with the high magnetic isotropy, this enables **1** to be an excellent magnetic refrigerant for low temperature applications.

Introduction

Magnetic refrigeration is a potential and realistic short-to-
15 medium term application envisioned for polymetallic molecules built from paramagnetic metal ions; molecules often referred to as molecular nanomagnets (MNMs).¹⁻³ The magnetocaloric effect (MCE) is based on the change of magnetic entropy upon application of a magnetic field and can
20 be used for cooling applications *via* adiabatic demagnetisation. Recent studies have demonstrated that the MCE of *isotropic* MNMs can be enormous,⁴⁻⁷ and larger than that of lanthanide alloys⁸ and magnetic nanoparticles.⁹ The “recipe” required for the synthesis of such molecules was recently outlined.¹⁰ The “ideal” molecule should possess: (a) a
25 large spin ground state, *S*. Magnetic entropy is related to *S* by $S_m = R \ln(2S + 1)$ [where *R* = gas constant] and thus the larger the *S* the larger the magnetic entropy. (b) Molecular isotropy ($D_{\text{cluster}} = 0$) – zero-field
30 splitting (anisotropy) orders molecular *M_s* levels, decreasing magnetic entropy changes. (c) High spin degeneracy – the presence of low-lying excited states is controlled by the exchange interaction (*J*) between metal ions. Weak exchange equates to multiple low-lying excited states each of which can
35 contribute to the magnetic entropy of the system via $S_m = R \ln(2S + 1)$. (d) A small molecular mass, *m_w*.

In other words we need to make low molecular mass ferro- or ferrimagnets displaying zero molecular anisotropy and exhibiting weak exchange interactions. This immediately points toward the
40 use of lanthanide ions and, in particular, the *f⁷* ion Gd³⁺ in the construction of homo- and heterometallic (Gd-3d) clusters. The inherently weak exchange mediated through the core-like *f*-orbitals of Gd³⁺ and its isotropic electronic configuration guarantee the presence of multiple low-lying [and hence field-
45 accessible] spin states, negating the need for ferromagnetic exchange in homometallic *f*-block clusters. Heterometallic complexes (e.g. Gd³⁺-Mnⁿ⁺, Gd³⁺-Cu²⁺ *etc*) can be guaranteed to afford non-zero spin ground states on account of their differing *d^{n/fⁿ}* electron configurations and on the basis of literature
50 precedents that show certain combinations, *e.g.* Gd³⁺-Cu²⁺, favour ferromagnetic exchange.¹¹ Molecular isotropy can be controlled in two ways: (a) through the use of isotropic metals ions (Gd³⁺,

Cu²⁺, Fe³⁺) since *D_{cluster}* is governed in the main by *d_{single ion}*, or (b) through the synthesis of highly symmetric molecules since
55 $D_{\text{cluster}} = 0$ in cubic (O_h, T_d) symmetry.

To date, the molecule with largest enhancement of the MCE is a mixed-valent [Mn^{II/III}₁₄] disc with values of $-\Delta S_m$ as large as 25 J Kg⁻¹ K⁻¹ for liquid-helium temperatures and $\Delta B_0 = 7$ T – almost a factor of 2 larger than that of [DyCo₂] nanoparticles.⁹
60 Herein we present the first Cu²⁺-Gd³⁺ candidate, by showing that [Cu^{II}₅Gd^{III}₄O₂(OMe)₄(teaH)₄(O₂CC(CH₃)₃)₂(NO₃)₄]·2MeOH·2Et₂O (1·2MeOH·2Et₂O) displays a truly enormous enhancement of the MCE with $-\Delta S_m$ reaching record values
65 larger than 30 J kg⁻¹ K⁻¹. This cluster forms part of a family of isostructural Cu^{II}₅Ln^{III}₄ clusters in which the anisotropic members, Ln = Tb, Dy and Ho, in contrast to Gd, display single molecule magnetism features (SMM).¹¹

Results and Discussion

70 The reaction of Cu(NO₃)₂·3H₂O and Gd(NO₃)₃·6H₂O with triethanolamine (teaH₃) and trimethylacetic acid in a basic alcoholic solution leads to the formation of blue crystals of [Cu^{II}₅Gd^{III}₄O₂(OMe)₄(teaH)₄(O₂CC(CH₃)₃)₂(NO₃)₄]·2MeOH·2Et₂O (1·2MeOH·2Et₂O).^{†‡} Compound **1** (Figure 1A)
75 crystallises in the triclinic space group *P-1* with the asymmetric unit containing half the cluster which lies upon an inversion centre. The complex contains five Cu^{II} (Cu1-Cu3 and symmetry equivalent, *s.e.*) and four Gd^{III} (Gd1, Gd2 and
80 *s.e.*) ions; the Cu^{II} ions forming a planar ‘bow-tie’ arrangement, with the four Gd^{III} ions forming a rectangle perpendicular to this (Figure 1B). The metallic skeleton thus describes four vertex and face-sharing {GdCu₃} tetrahedra (Figure 1C). Two central trigonal bipyramidal μ₅-O²⁻ ions (O1 and *s.e.*) link the perpendicular Cu₅ and Gd₄ frameworks
85 together. The central Cu^{II} ion (Cu1) is four coordinate and in a square planar geometry with a [CuO₄] coordination sphere. The outer four Cu^{II} ions (Cu2, Cu3 and symmetry equivalents) are also four coordinate and square planar but with [CuO₃N] coordination spheres and with an additional long (axial)
90 contact to a non-bonded O-atom (O13 and *s.e.*) of a teaH ligand (~2.4 – 2.7 Å). The Gd^{III} ions are eight coordinate and in distorted square antiprismatic geometries, with [GdO₈]

coordination spheres. The two carboxylates and four methoxide ions each bridge in a μ -fashion across the short edge of the Gd₄ rectangle, with one exception, O2(OMe⁻) and symmetry equivalent is μ_3 -bridging, the additional bond being to the central Cu^{II} ion. The NO₃⁻ ions each chelate to a Gd^{III} ion at the four “outer” corners of the Gd₄ rectangle. The doubly deprotonated $\mu_3:\eta^2:\eta^2:\eta^1:\eta^0$ teaH ligands each encapsulate one Cu^{II} ion using two O-atoms and one N-atom and then attach it to the long rectangular edge of the Gd₄ rectangle via their two μ -O-atoms. The non-bonding alcohol arms are protonated, two of which form H-bonds to solvent MeOH molecules and two of which form inter-molecular H-bonds to the NO₃⁻ ions of adjacent clusters. The latter interaction directs the formation 1-D H-bonded chains down the *c*-axis of the crystal.

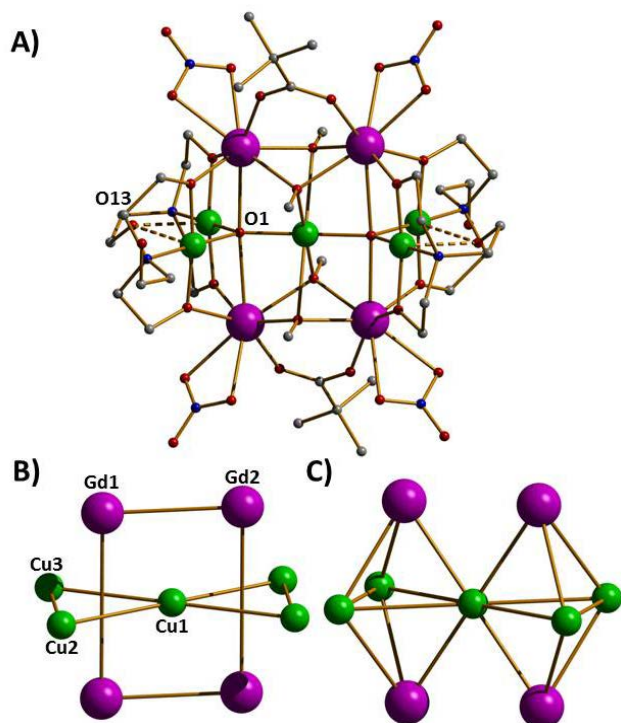


Fig. 1 A) The molecular structure of complex **1**. Colour code: Gd = purple, Cu = green, O = red, N = blue, C = grey. H-atoms are omitted for clarity. B) The metallic skeleton highlighting the two “interpenetrating” metal frameworks; the Cu₅ “bow-tie” and the Gd₄ rectangle. C) The metallic skeleton drawn to emphasise the four face- and vertex-sharing {Cu₃Gd} tetrahedra. The Gd...Gd distances across the short and long rectangular edges are 3.735 Å and 5.279 Å, respectively. The Cu1...Cu2,3 distances are ~3.5 Å; the Cu2...Cu3 distance is ~3.1 Å and the Cu...Gd distance, ~3.3 Å. Cu1-O1-Cu2, 123.88°, Cu1-O1-Cu3, 128.95°, Cu2-O1-Cu3, 107.05°.

The DC magnetic susceptibility of **1** was collected in an applied field $B_0 = 0.01$ T over the 2 – 300 K temperature range (Figure 2). The room-temperature $\chi_M T$ value of 33.0 cm³Kmol⁻¹ stays nearly constant with decreasing temperature down to ~30 K, below which it increases significantly reaching a value of 48.6 cm³ K mol⁻¹ at 2K, indicating that dominant ferromagnetic pathways are present. The $\chi_M T$ value expected for an uncoupled [Cu^{II}₅Gd^{III}₄] unit ($g = 2.00$) is

33.33 cm³ K mol⁻¹, in good agreement with the experimental data at high temperatures. The magnetisation measurements (inset of Figure 2) shows a saturation value of 31.3 $N\mu_B$, at the lowest investigated temperature $T = 2$ K, suggesting a net spin state $S = 31/2$. This can be rationalised assuming the central Cu^{II} to be antiferromagnetically coupled to the outer Cu sites in the ‘bow-tie’. This is likely to occur as the average Cu(central)-O-Cu(outer) bond angle is ~126° which will likely be antiferromagnetic and stronger than the outer Cu-O-Cu interactions (average angle of 107°) forcing the four Cu sites to align parallel to each other. The Cu...Gd interactions between the outer Cu ions and the Gd ions are likely weak and ferromagnetic, as has been noted for a number of Gd and Cu ions bridged by two O-atoms.¹² The weak exchange promoted by the lanthanide ions will most likely lead to several spin states energetically close to an ill-defined ground state, a sought after situation for observing an enhanced MCE.^{5-7,10}

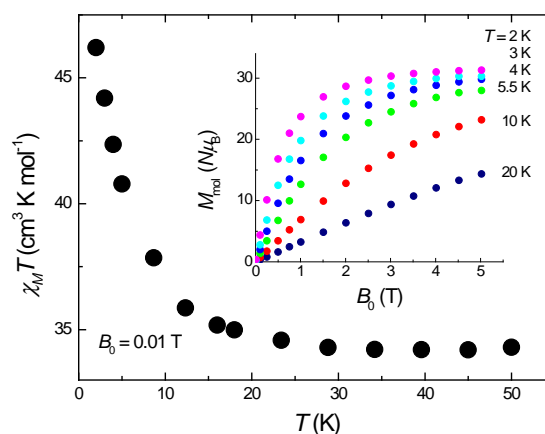
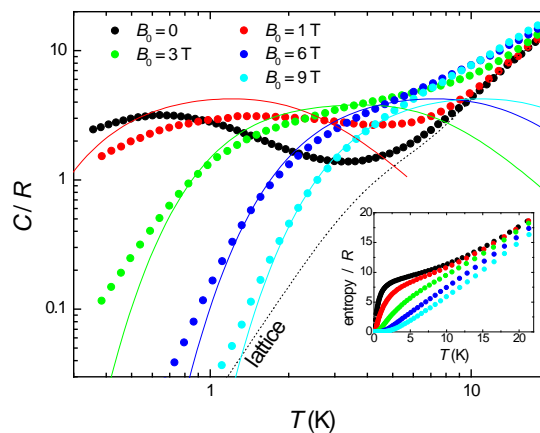


Fig. 2 Temperature-dependence of the $\chi_M T$ susceptibility of **1** collected for $B_0 = 0.01$ T. Inset: Field-dependence of the molar magnetisation for the indicated temperatures.

We next turn to the evaluation of the magnetothermal properties of **1** by presenting its temperature-dependent heat capacity (C) collected for several field values (Figure 3).

Fig. 3 Temperature-dependence of the heat capacity C normalised to



the gas constant R for **1** at several applied fields; the dotted line is the Debye fit to the lattice contribution, whereas the solid lines are the calculated Schottky contributions (see text). Inset: T -dependence of the entropy, as obtained from the C data.

At high temperatures, the heat capacity is dominated by a non-magnetic contribution arising from thermal vibrations of the lattice, which is modelled with the well-known low- T Debye function (dotted line in Fig. 3) yielding a value of $\Theta_D = 23$ K for the Debye temperature, typical for this class of cluster compound.¹ At low temperatures, the heat capacity is dependent upon the applied field. Indeed, the splitting of the molecular spin states results in a broad (Schottky-type) feature, which shifts to higher T by increasing the applied field. This behaviour can be explained using the same model which was suggested by the $M_{\text{mol}}(T, B_0)$ data, namely an antiferromagnetic core formed by the Cu^{II} spins (providing a net spin $S_{[\text{Cu}]} = 3/2$, $g = 2$ at low temperatures) that weakly couples to the peripheral Gd^{III} spins. As a comparison with the experimental data, Figure 3 shows the contributions (solid lines for $B_0 = 1, 3, 6$ and 9 T, respectively) that result by summing together the calculated Schottky curves arising from the field-split levels of a central $S_{[\text{Cu}]} = 3/2$ net spin and four independent Gd^{III} ($S = 7/2$, $g = 2$) spins. It can be seen that the higher fields promote a larger decoupling between the spin centres, yielding an increasingly much better agreement. The relatively poorer agreement at lower fields and temperatures can likely be ascribed to the presence of low-lying excited spin states, in accordance with the interpretation of the $M_{\text{mol}}(T, B_0)$ data. From the experimental heat capacity, the temperature dependence of the entropy is obtained by integration, *i.e.* using $\text{Entropy}(T) = \int C(T)/T dT$, and is depicted in the inset of Figure 3 for several applied fields. One can notice the $\sim 9 R$ “plateau” for the zero-field entropy in the $2 < T < 8$ K temperature range, which again can be understood within the frame of a model of four weakly coupled Gd^{III} spins to a central $S_{[\text{Cu}]} = 3/2$ core. Above $2 - 3$ K, the $\text{Cu}\dots\text{Gd}$ interactions are fully decoupled, therefore the expected entropy/ R should be $4 \times \ln(8) + \ln(4) = 9.7$, in agreement with the experimental value reached at the plateau. Above approximately 8 K, the zero-field entropy content increases steadily because of the dominant lattice heat capacity (see Figure 3).

We next evaluate the MCE of **1**, *i.e.* both the magnetic entropy change ΔS_m and adiabatic temperature change ΔT_{ad} from the temperature and field dependencies of the entropy.¹⁰ The results are summarised in Figure 4. We report a record value of $-\Delta S_m$ which reaches $\sim 31 \text{ J kg}^{-1} \text{ K}^{-1}$ at $T = 3$ K for $\Delta B_0 = 9$ T. This is what we could have expected considering the large net magnetic moment of the molecule, combined with the negligible anisotropy and the weak intra-cluster interactions that promote low-lying excited spin states.¹⁰ An added “pro” is the relatively small molecular mass ($m_w = 2141.8$ gr), which results from the small mass and relatively low ratio of ligands present. These being non-magnetic, contribute passively to the MCE. Likewise, the ΔT_{ad} is extraordinarily large (see bottom panel of Figure 4). We refer particularly to the cooling rate kelvin / tesla, which goes from more than 1 K/T for $\Delta B_0 = 9$ T to well over 2 K/T for $\Delta B_0 = 1$ T, setting this material among the most efficient refrigerants for the liquid-helium temperature range.¹⁰ Finally, we note an excellent agreement between the $-\Delta S_m$ obtained from the C data with that obtained by applying the Maxwell equation to the isothermal

magnetisation curves (the asterisks in Figure 4),¹⁰ suggesting that both independent procedures can be effectively used to characterise **1** with respect to its MCE.

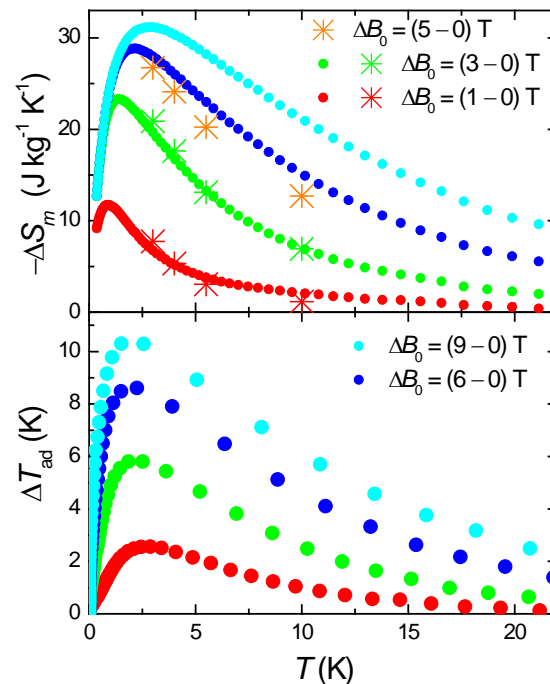


Fig. 4 Top: T -dependencies of the magnetic entropy change as obtained from C (filled dots) and M_{mol} (asterisks) experimental data, for the indicated applied field changes. Bottom: T -dependencies of the adiabatic temperature change obtained from C experimental data, for the indicated applied field changes.

Conclusions

The use of teH_3 in heterometallic $3d-4f$ chemistry has led to the isolation of an unusual but beautiful $[\text{Cu}^{\text{II}}_5\text{Gd}^{\text{III}}_4]$ cluster comprising a series of vertex- and face-sharing $\{\text{GdCu}_3\}$ tetrahedra. The low molecular mass, the constituent isotropic metal ions, the ferromagnetic $\text{Cu}^{\text{II}}-\text{Gd}^{\text{III}}$ interaction and the inherent weak exchange propagated by the lanthanide ions results in the population of numerous S states even at the lowest temperatures measured. This is reflected in a truly enormous enhancement of the MCE with $-\Delta S_m$ values larger than $30 \text{ J kg}^{-1} \text{ K}^{-1}$; the largest value seen for any molecular compound. This clearly demonstrates that $[\text{Cu}^{\text{II}}-\text{Gd}^{\text{III}}]$ cluster compounds – for so long studied because of the ferromagnetic exchange between the $3d$ and $4f$ metal ions – can be successfully exploited for magnetic refrigeration.

Acknowledgements

This work was supported by an ARC Discovery grant (KSM), the Spanish MICINN (contracts MAT2009-13977-C03 and CSD2007-00010); the EPSRC, Leverhulme Trust and Royal Society of Chemistry (EKB).

Notes and references

^aSchool of Chemistry, Monash University, Clayton, Victoria 3800,

Australia. E-mail: keith.murray@monash.edu

^bSchool of Chemistry, The University of Edinburgh, West Mains Road,

Edinburgh, EH9 3JJ (UK). E-mail: ebrechin@staffmail.ed.ac.uk

^cInstituto de Ciencia de Materiales de Aragón, CSIC-Universidad de

Zaragoza, Departamento de Física de la Materia Condensada, 50009

Zaragoza, Spain. E-mail: evange@unizar.es

$\dagger \ddagger [\text{Cu}^{\text{II}}_5\text{Gd}^{\text{III}}_4\text{O}_2(\text{teaH})_4(\text{O}_2\text{CC}(\text{CH}_3)_2(\text{NO}_3)_4(\text{OMe})_4)] \cdot 2\text{MeOH} \cdot 2\text{Et}_2\text{O}$
(**1**). $\text{Cu}(\text{NO}_3)_2 \cdot 3\text{H}_2\text{O}$ (0.2 g, 1 mmol) was dissolved in 20 ml of MeOH followed by the addition of triethanolamine (0.13 ml, 1 mmol), pivalic acid (0.05 g, 0.5 mmol) and triethylamine (0.5 ml, 3.5 mmol) to give a green/blue solution. To this $\text{Gd}(\text{NO}_3)_3 \cdot 6\text{H}_2\text{O}$ (0.45 g, 1 mmol) was added to give a deep blue solution. This was then stirred for 4 hours, allowed to stand and was then layered with diethyl ether. After 3 – 5 days blue crystals of **1** had formed. Yield: 102 mg, 39.2 %. Anal. Calculated (found) for **1**: $2\text{MeOH} \cdot 2\text{Et}_2\text{O}$: $\text{Cu}_5\text{Gd}_4\text{C}_{48}\text{H}_{110}\text{O}_{38}\text{N}_8$: C, 24.49 (24.20); H, 4.71 (4.29); N, 4.76 (4.59). Selected ATR IR data (cm^{-1}): 2957w, 2856s, 1559s, 1483s, 1457sh, 1423s, 1377w, 1360w, 1298s, 1251w, 1227w, 1155w, 1133w, 1083s, 1022s, 916m, 896m, 817w. X-Ray crystallographic measurements were performed at 100(2) K at the Australian synchrotron MX1 beam-line as described elsewhere.¹² The data collection and integration were performed within Blu-Ice¹³ and XDS¹⁴ software programs. The data collection and integration were performed within SMART and SAINT+ software programs, and corrected for absorption using the Bruker SADABS program. **1** was solved by direct methods (SHELXS-97) and refined (SHELXL-97) by full least matrix least-squares on all F^2 data.²⁶ Crystallographic details are available in the Supporting Information in CIF format. CCDC number 809026. These data can be obtained free of charge from the Cambridge Crystallographic Data Centre via www.ccdc.cam.ac.uk/data_request/cif. Crystal data for **1**:

M, g mol^{-1} = 2354.16, Crystal system = Triclinic, P-1, $a = 11.050(2)$, $b = 13.830(3)$, $c = 14.030(3)$ Å, $\alpha = 78.80(3)$, $\beta = 83.81(3)$, $\gamma = 69.28(3)^\circ$, $V/\text{Å}^3 = 1965.4(8)$, $T/\text{K} = 100(2)$, $Z = 1$, $\rho_{\text{calc}} [\text{g cm}^{-3}] = 1.989$, $\lambda_{\text{Cu}}/\text{Å} = 0.7182$, data measured = 12139, Ind. Reflns = 7056, $R_{\text{int}} = 0.0315$, Reflns with $I > 2\sigma(I) = 6876$, parameters = 477, restraints = 0, $R_1\text{c}$, $wR_2\text{c} = 0.0398$, 0.099, goodness of fit = 1.132, Largest residuals/ $e \text{ Å}^{-3} = 1.09$, -1.331.

- 1 M. Evangelisti, F. Luis, L. J. de Jongh and M. Affronte, *J. Mater. Chem.*, 2006, **16**, 2534.
- 2 M. Evangelisti, A. Candini, A. Ghirri, M. Affronte, E. K. Brechin and E. J. L. McInnes, *Appl. Phys. Lett.*, 2005, **87**, 072504.
- 3 R. Shaw, R. H. Laye, L. F. Jones, D. M. Low, C. Talbot-Eckelaers, Q. Wei, C. J. Milios, S. Teat, M. Helliwell, J. Raftery, M. Evangelisti, M. Affronte, D. Collison, E. K. Brechin and E. J. L. McInnes, *Inorg. Chem.*, 2007, **46**, 4968.
- 4 M. Manoli, R. D. L. Johnstone, S. Parsons, M. Murrie, M. Affronte, M. Evangelisti and E. K. Brechin, *Angew. Chem., Int. Ed.*, 2007, **46**, 4456.
- 5 M. Evangelisti, A. Candini, M. Affronte, E. Pasca, L. J. de Jongh, R. T. W. Scott and E. K. Brechin, *Phys. Rev. B: Condens. Matter Mater. Phys.*, 2009, **79**, 104414.
- 6 G. Karotsis, M. Evangelisti, S. J. Dalgarno and E. K. Brechin, *Angew. Chem., Int. Ed.*, 2009, **48**, 9928.
- 7 Y.-Z. Zheng, M. Evangelisti and R. E. P. Winpenny, *Chem. Sci.*, 2011, **2**, 99.
- 8 (a) V. K. Pecharsky and K. A. Gschneidner, Jr., *Phys. Rev. Lett.*, 1997, **78**, 4494. (b) F. X. Hu, B. G. Shen and J. R. Sun, *Appl. Phys. Lett.*, 2000, **76**, 3460. (c) F. X. Hu, B. G. Shen, J. R. Sun, Z. H. Cheng, G. H. Rao and X. X. Zhang, *Appl. Phys. Lett.*, 2001, **78**, 3675. (d) B. G. Shen, J. R. Sun, F. X. Hu, H. W. Zhang and Z. H. Chen, *Adv. Mater.*, 2009, **21**, 4545. (e) N. A. de Oliveira, P. J. von Ranke, M. V. Tovar Costa and A. Troper, *Phys. Rev. B: Condens. Matter Mater. Phys.*, 2002, **66**, 094402. (f) N. H. Duc, D. T. Kim Anh and P. E. Brommer, *Physica B*, 2002, **319**, 1. (g) N. K. Singh, P. Kumar, K. G. Suresh, A. K. Nigam, A. A. Coelho and S. Gama, *J. Phys.: Condens. Matter*,

2007, **19**, 036213. (h) H. Wada, Y. Tanabe, M. Shiga, H. Sugawara and H. Sato, *J. Alloys Compd.*, 2001, **316**, 245.

9 S. Ma, W. B. Cui, D. Li, N. K. Sun, D. Y. Geng, X. Jiang and Z. D. Zhang, *Appl. Phys. Lett.*, 2008, **92**, 173113.

75 10 M. Evangelisti and E. K. Brechin, *Dalton Trans.*, 2010, **39**, 4672.

11 S. K. Langley, L. Ungur, N. F. Chilton, B. Moubaraki, L. F. Chibotaru and K. S. Murray, in preparation.

12 See for example: (a) A. Benelli, C. Benelli, A. Caneschi, R. Carlin, A. Dei and D. Gatteschi, *J. Am. Chem. Soc.* 1985, **107**, 8128. (b) M. Andruh, I. Ramade, E. Codjovi, O. Guillou, O. Kahn and J. C. Trombe, *J. Am. Chem. Soc.*, 1993, **115**, 1823. (c) J. P. Costes, F. Dahan, A. Dupuis and J. P. Laurent, *Inorg. Chem.*, 1997, **36**, 3429. (d) A. J. Blake, R. O. Gould, C. M. Grant, P. E. Y. Milne, S. Parsons and R. E. P. Winpenny, *J. Chem. Soc., Dalton Trans.*, 1997, 485. (e) C. Benelli and D. Gatteschi, *Chem. Rev.*, 2002, **102**, 2369. (f) M. Evangelisti, M. L. Khan, J. Bartolomé, L. J. de Jongh, C. Meyers, J. Leandri, Y. Leroyer and C. Mathonière, *Phys. Rev. B: Condens. Matter Mater. Phys.*, 2003, **68**, 184405. (g) B. W. Wang, S. D. Jiang, X. T. Wang and S. Gao, *Sci. China Ser. B-Chem.*, 2009, **52**, 1739.

13 T. M. McPhillips, S. E. McPhillips, H. J. Chiu, A. E. Cohen, A. M. Deacon, P. J. Ellis, E. Garman, A. Gonzalez, N. K. Sauter, R. P. Phizackerley, S. M. Soltis and P. Kuhn, *J. Synchrotron Rad.*, 2002, **9**, 401.

95 14 W. Kabsch, *J. Appl. Crystallogr.*, 1993, **26**, 795.

15 (a) G. M. Sheldrick, SHELXL-97, Program for refinement of crystal structures, University of Göttingen, Germany, 1997. (b) A. L. Speck, *Acta. Crystallogr. Sect. A*, 1990, **46**, C34.